

Charged hadrons and nuclear parton distributions in p(d)A collisions

Adeola Adeluyi,¹ Trang Nguyen,² and Bao-An Li¹

¹*Department of Physics and Astronomy
Texas A&M University-Commerce, Commerce, TX 75429, USA*

²*Center for Nuclear Research, Department of Physics
Kent State University, Kent, OH 44242, USA*

(Dated: December 28, 2018)

Nuclear gluon modifications are the least constrained component of current global fits to nuclear parton distributions, due to the inadequate constraining power of presently available experimental data from nuclear deep inelastic scattering and nuclear Drell-Yan lepton-pair production. A recent advance is the use of observables from relativistic nucleus-nucleus collisions to supplement the data pool for global fits. It is thus of interest to investigate the sensitivity of various experimental observables to different strengths of nuclear gluon modifications from large to small Bjorken x . In this work we utilize three recent global fits with different gluon strengths to investigate the sensitivity of three observables: nuclear modification factor, pseudorapidity asymmetry, and charge ratio. We observe that both nuclear modification factor and pseudorapidity asymmetry are quite sensitive to the strength of gluon modifications in a wide pseudorapidity interval. The sensitivity is greatly enhanced at LHC (Large Hadron Collider) energies relative to that at RHIC (Relativistic Heavy Ion Collider). The charge ratio is mildly sensitive only at large Bjorken x . Thus measurement of these observables in proton-lead collisions at the LHC affords the potential to further constrain gluon modifications in global fits.

PACS numbers: 24.85.+p,25.30.Dh,25.75.-q

I. INTRODUCTION

Nuclear parton distribution functions (nPDFs) are an important ingredient in the theoretical description of nucleus-nucleus collisions using the framework of perturbative Quantum Chromodynamics (pQCD). Although the scale evolution of the nuclear parton distributions can be described perturbatively, nPDFs are intrinsically non-perturbative. This non-perturbative nature makes their theoretical determination from QCD hitherto intractable. Therefore, as obtains in the case of nucleon parton distribution functions (PDFs), the nPDFs are currently most efficiently determined from global fits to experimental data. Earlier global analyses [1–4] relied heavily on fixed-target nuclear deep-inelastic scattering (DIS) and Drell-Yan (DY) lepton-pair production, with the attendant low precision and almost total lack of constraints on nuclear gluon distributions. The use of an extended data set, incorporating data on inclusive hadron production in deuteron-gold collisions, has been pioneered in [5, 6], with better constraints on gluon modifications. Despite all these advances the nuclear gluon distribution is still the least constrained aspect of global fits to nPDFs.

Thus questions related to the distributions of partons (in particular gluons) in nucleons and nuclei remain of current interest, both theoretically and experimentally. Of particular importance are the marked suppression of the nuclear modification factor at forward rapidities and the issue of gluon saturation (see, for example [7, 8]). The Large Hadron Collider (LHC), even more than the Relativistic Heavy Ion Collider (RHIC), affords the opportunity to study several important aspects of these nuclear parton distributions in a center-of-mass energy and

transverse-momentum domain where pQCD is expected to work well. For precision tests of pQCD applied to nucleus-nucleus collisions and also for various other applications it is important to gain control over the uncertainties in the elucidation of nuclear gluon distributions. It is therefore beneficial to investigate the sensitivity of various observables to varying strengths of gluon modifications in different Bjorken- x regimes to further enhance the constraining ability of global fits.

In general the description of nuclear collisions based on pQCD is a complicated task. Much of the complication derives from the intrinsically complex nature of the nuclear environment in collisions of heavy nuclei. In addition to the initial-state modification of the PDFs, the cross section of high- p_T hadron production is influenced by final-state effects (such as jet energy loss) and a complicated geometry. To better understand the physics of pQCD in the nuclear environment, it is highly desirable to disentangle the different nuclear phenomena affecting high- p_T ($p_T \gtrsim 1.5$ GeV) hadron production. In this respect, asymmetric light-on-heavy nuclear collisions, such as p(d)A collisions offer the distinct advantage of absence of final-state effects. In fact, one of the physics goals of the Run 8 at RHIC was to provide a high-statistics “cold” nuclear matter data set to establish a definitive baseline for “hot” nuclear matter, created in gold-gold collisions. The benchmark role of the “the deuteron-gold control experiment” for e.g. energy-loss studies has often been emphasized [9, 10]. Proton-nucleus and deuteron-nucleus reactions have also been used to study the Cronin-effect [11, 12]. These asymmetric systems also offer unique information about the underlying dynamics not available in symmetric proton-

proton or nucleus-nucleus collision systems. For example, a new feature, offered by nonidentical colliding beams like d+Au, is the pseudorapidity asymmetry, examined in some detail by the STAR collaboration [13]. In view of the importance of asymmetric collisions, we anticipate similar pPb program at the LHC.

The strategy adopted in this study is as follows: we consider three global nuclear parton distribution sets [4–6] with different strengths of the nuclear gluon modifications. We are mainly interested in the sensitivity of observables to gluon modifications; therefore we consider these nPDF sets simply as sources of differing severity of gluon modifications. Further details about this aspect of the study are given in the next section. In order to avoid issues related to final-state effects which are present in nucleus-nucleus collisions, we limit our calculations to charged hadron production in both deuteron-gold collisions at RHIC and proton-lead collisions at the LHC. Utilizing this framework, we investigate the sensitivity of three basic quantities directly observable experimentally: the nuclear modification factor, the pseudorapidity asymmetry, and the charge ratio, to different strengths of the gluon modifications. The calculated results are compared with available experimental data: nuclear modification factor for charged hadrons from the BRAHMS Collaboration [14], and pseudorapidity asymmetry from the STAR Collaboration [13] respectively.

The paper is organized as follows: in Sec. II we review the basic formalism of the collinearly-factorized pQCD-improved parton model as applied to nucleus-nucleus collisions. This section also includes the definition of the minimum bias nuclear modification factor, pseudorapidity asymmetry, and charge ratio. We present the results of our calculations for these quantities in Sec. III. Our conclusion is contained in Sec. IV.

II. THEORETICAL FRAMEWORK AND EXPERIMENTAL OBSERVABLES

A. Collinear factorization

The minimum bias invariant cross section for the production of final hadron h from the collision of nucleus A (with mass number A) and nucleus B (with mass number B) ($A + B \rightarrow h + X$), can be written, in collinearly factorized pQCD, as

$$E_h \frac{d^3\sigma_{AB}^h}{d^3p} = AB \sum_{abcd} \int dx_a dx_b dz_c F_{a/A}(x_a, Q^2) \\ \times F_{b/B}(x_b, Q^2) \frac{d\sigma(ab \rightarrow cd)}{d\hat{t}} \\ \times \frac{D_{h/c}(z_c, Q_f^2)}{\pi z_c^2} \hat{s} \delta(\hat{s} + \hat{t} + \hat{u}) \quad (1)$$

Here x_a and x_b are parton momentum fractions in A and B , respectively, and z_c is the fraction of the parton momentum carried by the final-state hadron h . The

factorization and fragmentation scales are denoted as Q and Q_f , respectively. As usual, \hat{s} , \hat{t} , and \hat{u} refer to the partonic Mandelstam variables, and the massless parton approximation is used in this study as expressed in the delta function. The quantity $d\sigma(ab \rightarrow cd)/d\hat{t}$ in Eq. (1) represents the perturbatively calculable partonic cross section, and $D_{h/c}(z_c, Q_f^2)$ stands for the fragmentation function of parton c to produce hadron h , evaluated at momentum fraction z_c and fragmentation scale Q_f . For a recent discussion on the issue of collinear factorization in nucleus-nucleus collision see [15].

The homogeneous nuclear parton distribution functions (nPDFs) $F_{a/A}(x, Q^2)$, for a nucleus with N neutrons and $Z = A - N$ protons, with A the mass number, can in general be written as

$$F_{a/A}(x, Q^2) = \frac{Z}{A} f_{a/p/A}(x, Q^2) + \frac{N}{A} f_{a/n/A}(x, Q^2) \\ = (1 - \omega) f_{a/p/A}(x, Q^2) + \omega f_{a/n/A}(x, Q^2) \quad (2)$$

with $\omega = N/A$ and $0 \leq \omega \leq 1$. The function $f_{a/p/A}(x, Q^2)$ denotes the parton distribution for parton a in a bound proton in nucleus A and $f_{a/n/A}(x, Q^2)$ the distribution in a bound neutron respectively, and are related, for valence quarks, by isospin symmetry. They are expressible as convolutions of free nucleon parton distribution functions (PDFs) $f_{a/N}(x, Q^2)$ and a shadowing function $S_{a/A}(x, Q^2)$ which encodes the nuclear modifications of parton distributions in nucleus A . We employ three different nuclear parton distributions in this study: the HKN07 [4] ("weak" gluon modifications), the EPS08 [5] ("strong" gluon modifications), the EPS09 [6] ("moderate" gluon modifications) sets. Note that for HKN07 and EPS09 the qualifiers "weak" and "moderate" respectively are with respect to the central fits; inclusion of uncertainties generates considerable spread in the relative measure of gluon modifications. For consistency reasons we use the underlying nucleon PDFs employed in the HKN07 nPDFs, namely MRS98 [16]. The results are quite insensitive to the choice of nucleon PDFs in general. For the final hadron fragmentation we utilize the fragmentation functions in the DSS07 set [17]. The factorization scale as well as the fragmentation scale are set to evolve with the transverse momentum of the outgoing hadron, according to $Q = Q_f = p_T$. Since pQCD calculations are generally not reliable at very low p_T , the lower limit on our calculations has been set to $p_T = 1.5$ GeV/c. With our scale choice, this corresponds to a minimum Q^2 (Q_f^2) of 2.25 GeV 2 , while EPS08, EPS09, and HKN07 give 1.69, 1.69, and 1.0 GeV 2 for minimum Q^2 , respectively. The minimum Q_f^2 for the DSS fragmentation functions is given as 1.0 GeV 2 .

It should be noted that whereas both EPS09 and HKN07 are available in both leading order (LO) and next-to-leading order (NLO) parametrizations, EPS08 is available only in leading order. Our calculations are therefore to leading order. Since we consider charged hadrons, we need charge-separated fragmentation functions. These fragmentation functions are also available

at LO and NLO, with the NLO set adjudged more accurate [17]. We have performed calculations using both, and the results presented here are for the NLO set. The implication of using NLO fragmentation functions in a LO calculation is treated in [18].

A comprehensive treatment of the uncertainties on calculated results has not been undertaken in the present study. The overall uncertainties on the calculated results obviously depend on three components: the nPDFs, truncation of the perturbative series for the hard partonic cross sections, and the charged hadron fragmentation functions. Although both EPS09 and HKN07 have facilities for estimating the uncertainties in the nPDFs, we have not included these uncertainties in our calculations. We have used the central fits in these two routines without recourse to their associated uncertainties. While the inclusion of uncertainties may be important for comparing the relative efficacy of different nPDFs, the focus here is on the sensitivity of the observables to different gluon modification scenarios. It is thus more transparent for the purpose at hand to use the central fits in HKN07 and EPS09, but bearing in mind the potential overlap of calculated results with the inclusion of uncertainties in these nPDFs. The calculated quantities in the present study are ratios, therefore truncation errors largely cancel (for a comparison of LO and NLO nuclear modification factor, see, for instance, [2]). The errors arising from fragmentation functions are basically unknown.

B. Nuclear modification factor

The minimum bias nuclear modification factor compares, as a ratio, spectra of particles produced in nuclear collisions to a hypothetical scenario in which the nuclear collision is assumed to be a superposition of the appropriate number of proton-proton collisions. The ratio can be defined as a function of p_T for any produced hadron species h at any pseudorapidity η :

$$R_{AB}^h(p_T, \eta) = \frac{1}{AB} \cdot \frac{E_h d^3 \sigma_{AB}^h / d^3 p}{E_h d^3 \sigma_{pp}^h / d^3 p} \quad (3)$$

Nuclear effects manifest themselves in $R_{AB}^h(p_T)$ values greater or smaller than unity, representing enhancement or suppression, respectively, relative to the pp reference.

The determination of the nuclear modification factor involves the cross section for proton-proton collisions in the denominator, and is thus sensitive to the precision of the knowledge of the pp cross section. The other two observables considered, the pseudorapidity asymmetry and charge ratio, are independent of a baseline pp cross section and therefore do not suffer from this constraint.

C. Pseudorapidity asymmetry

In general, as the mechanisms for hadron production in $p(d)A$ collisions may be different at forward rapidities

($p(d)$ side) and backward rapidities (A side), it is of interest to study ratios of particle yields between a given pseudorapidity value (interval) and its negative in these collisions. Thus the pseudorapidity asymmetry, Y_{AB}^h , is defined as the ratio of the yield in the backward (“target-side”, negative rapidities) region relative to the yield in the forward (“projectile-side”, positive rapidities) region:

$$Y_{AB}^h(p_T) = E_h \frac{d^3 \sigma_{AB}^h}{d^3 p} \Big|_{-\eta} \Big/ E_h \frac{d^3 \sigma_{AB}^h}{d^3 p} \Big|_{\eta} . \quad (4)$$

The meaning of the pseudorapidity asymmetry is clear: a ratio greater than unity implies more yield in the backward (A side) region relative to the forward ($p(d)$) region while a ratio less than unity implies the converse. Since the nPDFs are an important ingredient in hadron production, the study of pseudorapidity asymmetry can offer valuable information in further constraining the nuclear parton distributions. As remarked above, the pseudorapidity asymmetry is independent of a reference pp cross section and thus more “self-contained”; it is also more global in the sense that it encapsulates information on nPDFs at different Bjorken- x values. For conciseness, we will refer to $Y_{AB}^h > 1$ as positive asymmetry and $Y_{AB}^h < 1$ as negative asymmetry.

D. Charge ratio and rapidity asymmetry of charge ratio

Let us define the charge ratio as the ratio of the yield of negatively charged hadrons to the yield of the positively charged hadrons. Then we have

$$Z_{AB}^h(p_T, \eta) = E_h \frac{d^3 \sigma_{AB}^h}{d^3 p} \Big|_{h=h^-} \Big/ E_h \frac{d^3 \sigma_{AB}^h}{d^3 p} \Big|_{h=h^+} . \quad (5)$$

The charge ratio is expected to be more sensitive to the fragmentation functions than to the nuclear parton distributions, especially as one moves toward forward (large positive) rapidities. Nevertheless, in the backward direction (negative rapidities) and even near midrapidity, the charge ratio shows some sensitivity to nuclear parton distributions. This rapidity dependence is conveniently displayed in terms of a pseudorapidity asymmetry of the charge ratio, $Y_Z^{AB}(p_T)$, defined as the ratio of the charge ratio at negative rapidities relative to that at positive rapidities. Technically this is equivalent to the ratio of the pseudorapidity asymmetry of negatively charged hadrons relative to the asymmetry of the positively charged hadrons:

$$Y_Z^{AB}(p_T) = Z_{AB}^h(p_T, \eta) \Big|_{-\eta} \Big/ Z_{AB}^h(p_T, \eta) \Big|_{\eta} . \quad (6)$$

III. RESULTS

The gluon distribution is the least constrained, and therefore, constitute the largest source of differences be-

tween the various global fits to nuclear parton distributions (see [6, 19]). Thus the differences in the predictions of the three sets under consideration stem largely from the differences associated with their respective gluon modifications. These differences are largest at the initial factorization scale ($Q_0^2 = 1.69, 1.0$ GeV 2 for both EPS08 and EPS09, and HKN07 respectively) and decreases with increasing Q^2 due to evolution. With our choice of scales ($Q = Q_f = p_T$) the results presented here are sensitive to these differences up to the highest p_T considered, $p_T = 60$ GeV.

Nuclear effects encoded in the nPDFs are x -dependent, and thus different effects are present at different x : shadowing ($x \lesssim 0.1$, depletion), antishadowing ($0.1 \lesssim x \lesssim 0.3$, enhancement), EMC effect ($0.3 \lesssim x \lesssim 0.8$, depletion), and Fermi motion ($x > 0.1$, enhancement). Due to the x_b -integration in Eq. (1) ($x_{min}^B(p_T, \eta) \leq x_b \leq 1$), different nuclear effects are superimposed, thus it is difficult to effect a puritanical isolation of these different nuclear effects.

In the following subsections we present the results of our calculations for nuclear modification factor, pseudorapidity asymmetry, and charge ratio for the production of charged hadrons in dAu collisions at RHIC and pPb collisions at the LHC. It should be emphasized that the results from both HKN07 and EPS09 nPDFs are from their respective central fits.

A. Nuclear modification factor of charged hadrons at RHIC and the LHC

1. Charged hadron modification factor at RHIC

In Figure 1 we present our result for nuclear modification factor of charged hadrons at RHIC. Data exist for negatively charged hadrons at forward rapidities and for sum of charged hadrons around midrapidity, and the level of agreement of calculation with data is as shown in the figure. Our calculations extends over the positive and negative BRAHMS pseudorapidity intervals ($-3.5 < \eta < 3.5$), and thus cover reasonably well the whole spectrum of nuclear effects, viz, shadowing, antishadowing, EMC effects and Fermi motion. As is well known, large backward (negative) rapidities correspond to large Bjorken- x momentum fractions in the gold nucleus while large forward (positive) rapidities correspond to small Bjorken- x momentum fractions. Thus as we move from backward to forward different nuclear effects come into play: from EMC/Fermi motion effects at large x to progressively stronger suppression due to nuclear shadowing at very small Bjorken- x . A major limitation at RHIC is that the kinematics are such that the very small x region ($x << 0.1$) is not appreciably accessed, except at very small p_T , where soft physics effects could be significant. This constraint is alleviated at LHC energies where it is possible to access the low x even at relatively high p_T .

A further complication is the presence of strong isospin effects on the nuclear modification factor of charged hadrons in deuteron-gold collisions, in particular at very forward rapidities. This is readily apparent from the appreciably different modification factors at forward rapidities for positively charged and negatively charged hadrons respectively, in contrast with the equality of these modification factors at forward rapidities in proton-nucleus collisions. These effects are somewhat minimized for the sum of charged hadrons, especially about midrapidity ($-1.2 < \eta < 1.2$), and so we therefore illustrate the influence of nuclear effects on the nuclear modification factor of sum of charged hadrons.

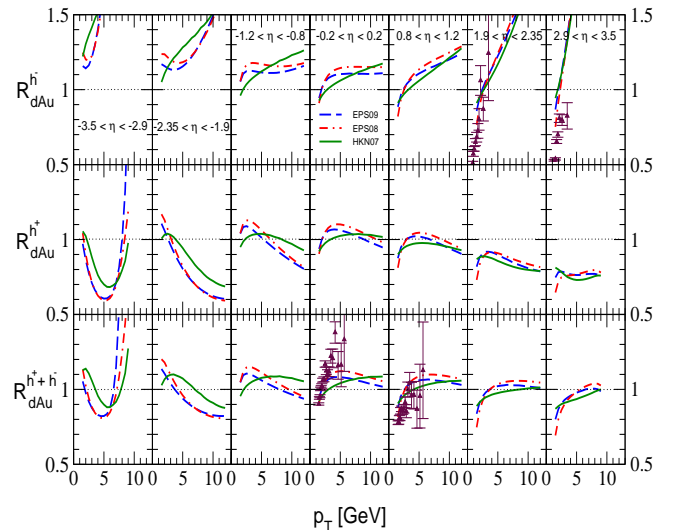


FIG. 1: (Color Online) Nuclear modification factor, R_{dAu} , for charged hadron production in d+Au collisions at RHIC ($\sqrt{s_{NN}} = 200$ GeV) from backward ($\eta = -3.5$) to forward ($\eta = 3.5$) pseudorapidities. The solid line represents the HKN07 nPDFs, the dashed line the EPS09 nPDFs, while the dot-dashed line represents the EPS08 nPDFs. The filled triangles denote the BRAHMS data [14].

Very backward rapidities ($-3.5 < \eta < -2.9$): at the lowest p_T considered ($p_T \sim 1.5$), $x_{min}^{Au} \sim 0.2$, and thus the modification factor is determined by the relative contributions from antishadowing, EMC effect, and Fermi motion, leading to $R_{dAu} > 1$. As p_T increases, x_{min}^{Au} becomes larger and therefore only the EMC effect and Fermi motion contribute, with $R_{dAu} < 1$. Finally, at sufficiently high p_T , only the Fermi motion is present, thus leading to an enhancement ($R_{dAu} > 1$).

Backward rapidities ($-2.35 < \eta < -0.8$): at very low p_T , x_{min}^{Au} is in the region of the advent of shadowing for $-2.35 < \eta < -1.9$, and already in the shadowing region for $-1.2 < \eta < -0.8$ respectively. Thus there is

full contribution from antishadowing (enhancement) for $-2.35 < \eta < -1.9$ and some shadowing (suppression) for $-1.2 < \eta < -0.8$. At intermediate p_T s there are contributions from both antishadowing and the EMC/Fermi motion. For the interval $-2.35 < \eta < -1.9$ the antishadowing contribution becomes negligible for $p_T > 5$ GeV, while it is still present though small even at high p_T for $-1.2 < \eta < -0.8$. At high p_T the modification factor is influenced dominantly by the EMC effect.

Midrapidities ($-0.2 < \eta < 0.2$): shadowing contributes appreciably at very low p_T with negligible contributions at higher p_T . The physics at intermediate and higher p_T is determined by the relative contributions from antishadowing (particularly for $p_T < 7.5$) and the EMC effect.

Forward rapidities ($0.8 < \eta < 2.35$): shadowing contributes significantly at very low p_T for $0.8 < \eta < 1.2$ and up till around $p_T \sim 3$ GeV for $1.9 < \eta < 2.35$, although the effect is more pronounced at lower p_T . The modification factor at higher p_T is determined by a mix of antishadowing and the EMC/Fermi motion.

Very forward rapidities ($2.9 < \eta < 3.5$): here shadowing dominates at very low p_T and the effect persists up to $p_T \sim 4$ GeV. The effect of antishadowing is seen in the rise of R_{dAu} between 4 and 8 GeV while the EMC effect is responsible for the downward trend of R_{dAu} at $p_T > 8$ GeV.

This simple analysis using the x -dependence of nuclear effects is of course modified for positively and negatively charged hadrons respectively. For negatively charged hadrons, the net effect is a rapid enhancement of the modification factor with p_T , especially at very backward and forward rapidities, and a less steep enhancement with p_T around midrapidities. The converse is the case for positively charged hadrons, although the suppression is less steep with increasing p_T at both backward and forward rapidities.

The observed predictions of the three different nPDFs sets reflect the different relative strengths of the nuclear effects encoded in these nPDFs, especially the nuclear gluon modifications. Even though there are clear differences between the predictions of EPS09/EPS08 relative to those of HKN07 across board, a reflection of strong versus weak gluon modifications, the distinction between EPS08 and EPS09 is not very apparent at the very backward and very forward rapidities, except at low p_T . In the interval $-2.35 < \eta < 2.35$, due to different gluon antishadowing and EMC, the distinction is more appreciable, despite the similarity in shape of the modification factor. The kinematics at the LHC will permit going deep into the shadowing regime at forward rapidities, and thus one anticipates clear-cut distinctions in the predictions of EPS08 and EPS09 nPDFs for significant range of p_T .

We now compare our results with experimental data. The BRAHMS Collaboration [14] has measured nuclear modification factor for sum of charged hadrons in the intervals $-0.2 < \eta < 0.2$ and $0.8 < \eta < 1.2$, and for negatively charged hadrons in the intervals $1.9 < \eta < 2.35$

and $2.9 < \eta < 3.5$. Figure 1 shows our result for both negatively charged hadrons and sum of charged hadrons for the relevant η intervals. The effect of the different gluon modifications present in the three nPDFs is apparent: EPS08 consistently has the strongest suppression at very low p_T , while HKN07 has the weakest, for all pseudorapidity intervals. The effect of gluon antishadowing and EMC is also readily seen for both $-0.2 < \eta < 0.2$ and $0.8 < \eta < 1.2$. In the interval $-0.2 < \eta < 0.2$, EPS08, due to its stronger gluon modifications, has the best agreement with data ($p_T < 6$ GeV) while HKN07 has the least. All three nPDFs are in good agreement with data for both $0.8 < \eta < 1.2$ and $1.9 < \eta < 2.35$, although the reach of the data is quite limited for the latter interval.

At very forward rapidities ($2.9 < \eta < 3.5$) the data show a suppression for the yield of negatively charged hadrons not adequately reproduced by calculations for $p_T > 2$ GeV, albeit with the small reach in p_T . This suppression has generated a lot of interest, with diverse mechanisms being proffered to explain the phenomenon (see, for instance, [20–23]. Since our purpose here is to compare predictions from different nPDFs, we will not go into discussions of the various explanations of the observed suppression. Some earlier studies of nuclear modification factor with different nPDFs can be found in [21, 24–26].

2. Charged hadrons modification factor at the LHC

We now consider nuclear modification factor of charged hadrons in proton-lead collisions at the LHC. Figure 2 shows our results for positively charged, negatively charged, and sum of charged hadrons. Unlike what obtains in deuteron-gold collisions, the modification factors for positively and negatively charged hadrons are the same, except at very backward rapidities ($\eta = -6$ and $\eta = -4$) where isospin effects in the Pb nucleus are appreciable, and the comments above applicable. The behavior of the modification factor across the spectrum of pseudorapidities mirrors the trend seen in d+Au collisions. We illustrate this for the sum of charged hadrons at the very backward rapidity.

At $\eta = -6$ and $p_T = 1.5$ GeV, $x_{min}^{Pb} \sim 0.07$ and thus there is negligible contribution from shadowing. The modification factor thus reflects the competing contributions from antishadowing/Fermi motion (enhancement) and the EMC effect (suppression). Higher transverse momenta translate to larger x_{min}^{Pb} , with less contribution from antishadowing, leading to $R_{pPb} < 1$. With $p_T > 10$ GeV, the dominant contribution is from Fermi motion, with the attendant $R_{pPb} > 1$.

The major difference is the accessibility of the small- x region even at backward rapidities and at relatively high transverse momenta for both midrapidities and forward rapidities. For instance, at $\eta = -2$ and $p_T = 10$ GeV, $x_{min}^{Pb} \sim 0.01$, well within the shadowing region while at

$\eta = 2$ and $p_T = 60$ GeV, $x_{min}^{Pb} \sim 0.001$, signifying a substantial contribution from shadowing at this relatively high p_T . In fact, at very forward rapidities ($\eta = 4, 6$) the influence of shadowing is so strong as to render $R_{pPb} < 1$ for all p_T considered. The strong sensitivity of the nuclear modification factor to gluon modifications enables a clear distinction of the predictions of the three nPDFs sets utilized in this study.

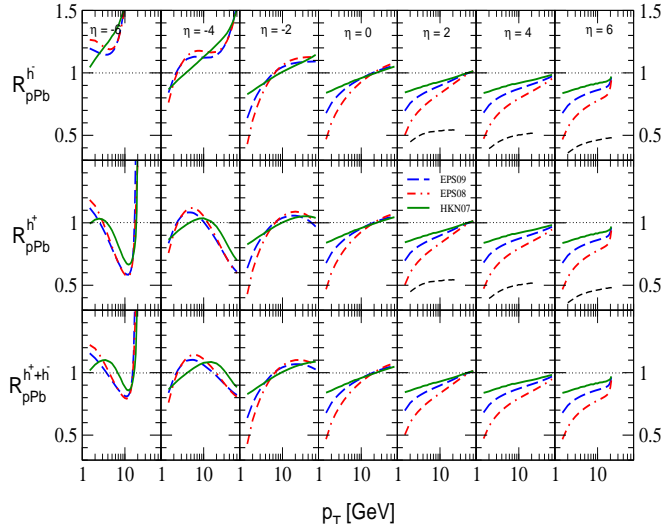


FIG. 2: (Color Online) Nuclear modification factor, R_{pPb} , for charged hadron production in $p+Pb$ collisions at the LHC ($\sqrt{s_{NN}} = 8.8$ TeV) from backward ($\eta = -6$) to forward ($\eta = 6$) pseudorapidities. The solid line represents the HKN07 nPDFs, the dashed line the EPS09 nPDFs, while the dot-dashed line represents the EPS08 nPDFs. The short dashed line is the result from a recent Color Glass Condensate (CGC) calculation [27].

The Color Glass Condensate (CGC) is an attractive framework for addressing forward rapidity (small- x) physics (for a recent review see [7]). For comparison purposes we show the predicted nuclear modification factor for charged hadrons at rapidities $y = 2, 4, 6$ from a recent calculation [27] in this framework. Our result shows less suppression and a more dramatic p_T dependence than the CGC.

B. Pseudorapidity asymmetry of charged hadrons at RHIC and the LHC

We now address pseudorapidity asymmetry in $d+Au$ collisions at RHIC and $p+Pb$ collisions at the LHC. A transparent way to understand the p_T dependence of pseudorapidity asymmetry is to consider the asymmetry

as a ratio of backward and forward nuclear modification factors [28], the pp cross section being symmetric with respect to pseudorapidity. Thus it is rather straightforward to apply the preceding analysis of the nuclear modification factor using the x dependence of nuclear effects to the p_T dependence of pseudorapidity asymmetry. Pseudorapidity asymmetry has been studied for different asymmetric systems and at different energies in [26, 28–31]

1. Asymmetry at RHIC

In Figure 3 we present the pseudorapidity asymmetry for charged hadrons and sum of charged hadrons produced in deuteron-gold collisions at RHIC. In the interval $0.8 < |\eta| < 1.2$ the calculated asymmetry is practically the same for both positively and negatively charged hadrons, and by implication, the sum of charged hadrons. For $p_T < 6$ GeV both EPS09 and EPS08 yield a positive asymmetry (> 1), with the EPS08 giving a larger asymmetry especially at low transverse momenta due to the stronger gluon modifications. Above $p_T = 6$ GeV, the two nPDFs set predict a negative asymmetry (< 1) of essentially the same magnitude. The effect of a rather weak gluon modification in HKN07 is apparent: the predicted asymmetry at low p_T is less than that of both EPS08 and EPS09. In fact, the predicted asymmetry is positive for all transverse momentum considered, with the asymmetry essentially unity at large p_T . The result for the sum of charged hadrons is compared with the available experimental data from the STAR Collaboration [13] for the interval $0.5 \leq |\eta| \leq 1.0$. Since this interval is not far from midrapidity, the calculated asymmetry is rather weak, in agreement with experimental observation [32, 33].

Larger asymmetries are expected as we move away from midrapidity. This is readily apparent in the interval $1.9 < |\eta| < 2.35$ where the calculated asymmetries for all three nPDFs sets are quite significant. While HKN07 predicts essentially the same asymmetry for both charge specie and the sum of charged hadrons, both EPS09 and EPS08 predict, at higher transverse momenta, a larger negative asymmetry for the positively charged hadrons relative to the negatively charged hadrons. The effect of the different nuclear gluon modifications in the three nPDFs is also apparent: EPS08 yields the largest positive (negative) asymmetry at low (high) p_T while HKN07 yields the smallest, especially for positively charged hadrons and sum of charged hadrons. Also there are small but discernible differences between EPS09 and EPS08 for all transverse momenta, unlike the case for the interval $0.8 < |\eta| < 1.2$ where both predict the same asymmetry for $p_T > 6$ GeV. Whereas both EPS09 and EPS08 yield positive asymmetry for $p_T < 4$ GeV and negative for $p_T > 4$ GeV, HKN07 gives negative asymmetry only for $p_T > 7$ GeV.

The above observations are also relevant for the asymmetries from the three sets in the interval $2.9 < |\eta| < 3.5$.

2. Asymmetry at the LHC

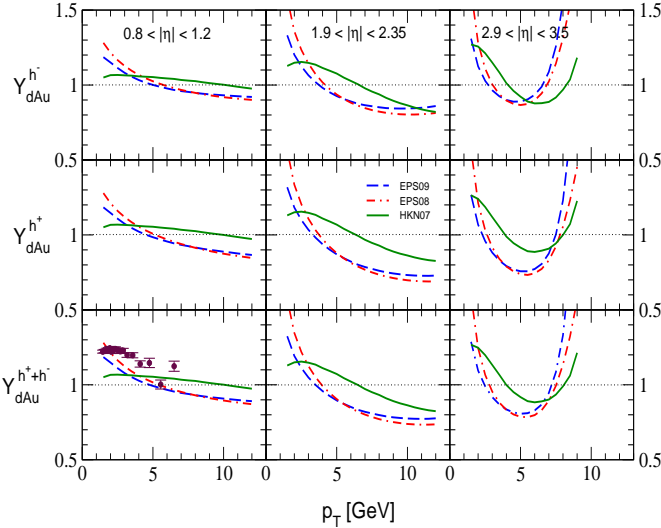


FIG. 3: (Color Online) Pseudorapidity asymmetry, Y_{dAu} for charged hadrons at $0.8 < |\eta| < 1.2$, $1.9 < |\eta| < 2.35$, and $2.9 < |\eta| < 3.5$ from d+Au collisions at RHIC ($\sqrt{s_{NN}} = 200$ GeV). The solid line represents the HKN07 nPDFs, the dashed line the EPS09 nPDFs while the dot-dashed line corresponds to the EPS08 nPDFs. The filled circles denote the STAR data [13] for $0.5 \leq |\eta| \leq 1.0$.

The difference between EPS09 and EPS08, though small, is quite distinct for all charged species and at all relevant p_T . Both predict more significant asymmetry for positively charged hadrons than for negatively charged hadrons and for sum of charged hadrons. The physics of the asymmetry (a ratio) in this interval is governed largely by shadowing/antishadowing (denominator) and EMC/Fermi motion (numerator). Thus both EPS08 and EPS09 predict negative asymmetry for $2.8 < p_T < 7.5$ GeV and positive everywhere else. On the other hand, HKN07 yields a positive asymmetry for $p_T < 4.5$ GeV and $p_T < 8.5$ GeV, with negative asymmetry for transverse momenta within these bounds.

It is pertinent to remark at this stage that even though the predictions from EPS08/EPS09 on the one hand, and those of HKN07 on the other hand are clearly distinguishable, the kinematic reach at RHIC is such as to limit the clarity of the distinction between a strong gluon modification scenario as present in EPS08 and the somewhat more moderate gluon modification as in EPS09. The kinematics at the LHC allow such a distinction, and thus the study of pseudorapidity asymmetry at the LHC may shed some light on the actual strength of nuclear gluon modifications.

Figure 4 depicts our result for pseudorapidity asymmetry of charged hadrons at the LHC. Let us consider the first interval: $|\eta| = 2$. Even at this relatively small pseudorapidity the different predictions of the three nPDFs are clearly distinguishable. Both EPS09 and EPS08 predict a negative asymmetry for $p_T < 2$ GeV, with the EPS08 yielding about twice the value of EPS09 at the lowest p_T considered. Thereafter both predict a positive asymmetry which peaks around $p_T = 9$ GeV and then decreases towards unity at very high p_T . At this peak, EPS08 yields an asymmetry of about 30% while EPS09 yields about 20%. The asymmetry predicted by HKN07 is characteristically different: it rises approximately monotonically as p_T increases and is positive for all p_T considered. At the highest p_T considered ($p_T = 60$ GeV), the asymmetry predicted by HKN07 is roughly the same as EPS08 for both negatively charged hadrons and sum of charged hadrons, and about 15% greater for positively charged hadrons. From Figure 4 it is apparent that the region $3 < p_T < 20$ GeV gives the best discriminatory ability for the considered pseudorapidity.

The distinguishability of the different predictions of pseudorapidity asymmetry by the three nuclear parton distributions sets is appreciably magnified for the interval $|\eta| = 4$, especially for $p_T < 20$ GeV. In this p_T region the predicted asymmetries are positive and approximately independent of the charge specie, with EPS08 giving the largest asymmetry and HKN07 the smallest. Above this region the predicted asymmetries are positive for negatively charged hadrons and gradually turn negative and close in magnitude as p_T increases for positively charged hadrons and sum of charged hadrons. Thus the region $p_T < 15$ GeV affords the best opportunity to discriminate between the different scenarios of gluon modifications as enshrined in the three nPDFs.

The above observations for $|\eta| = 4$ apply equally well for the pseudorapidity asymmetry in the interval $|\eta| = 6$. Here, due to phase space limitations, good discriminatory ability is limited to the transverse momentum region $p_T < 10$ GeV. While the predicted asymmetries remain positive for all p_T in the case of negatively charged hadrons, positively charged hadrons (sum of charged hadrons) exhibit a crossover from positive asymmetry to negative asymmetry around $p_T = 6$ GeV ($p_T = 10$ GeV) and a sharp rise back to positive asymmetry at around $p_T = 15$ GeV.

Thus contrary to what obtains at RHIC energies, pseudorapidity asymmetry at the LHC offers the potential of clearly distinguishing between various nPDFs with different nuclear gluon modifications.

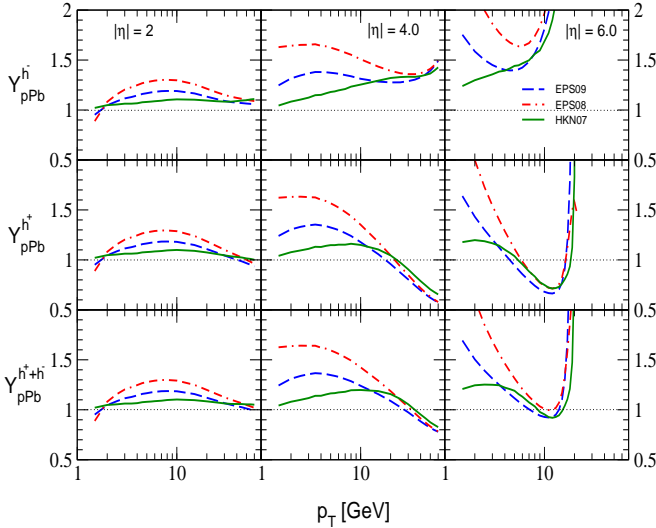


FIG. 4: (Color Online) Pseudorapidity asymmetry, Y_{pPb} for charged hadrons at $|\eta| = 2$, $|\eta| = 4$, and $|\eta| = 6$ from p+Pb collisions at the LHC ($\sqrt{s_{NN}} = 8.8$ TeV). The solid line represents the HKN07 nPDFs, the dashed line the EPS09 nPDFs while the dot-dashed line corresponds to the EPS08 nPDFs.

C. Charge ratio and its asymmetry at RHIC and the LHC

The top panel of Figure 5 shows the result of our calculation of the charge ratio in d+Au collisions at RHIC. The ratio is consistently below unity for all η intervals and transverse momenta considered, with the implication of a suppression of negatively charged hadrons relative to the positively charged hadrons, in accord with expectations from fragmentation. The suppression is smallest around midrapidity where the charge ratio is close to unity, and becomes progressively more enhanced as one moves towards larger negative and positive rapidities. In the very backward rapidity interval considered ($-3.5 < \eta < -2.9$), the sensitivity of the charge ratio to nPDFs is most pronounced. While both EPS09 and EPS08 manifest practically the same behavior, HKN07 displays a greater suppression than both EPS09 and EPS08. This difference decreases significantly as we move towards positive rapidities, such that already at the interval $0.8 < \eta < 1.2$ all three nPDFs exhibit the same behavior for the charge ratio. Thus at very forward rapidities the charge ratio is independent of the differences in the nuclear parton distributions, and is thus solely determined by the fragmentation functions.

The same trend is observed for p+Pb collisions at the LHC. Both EPS09 and EPS08 predict essentially the same behavior for all rapidities and transverse momenta.

As in the case of d+Au collisions at RHIC, the sensitivity is most pronounced for the very backward pseudorapidities and disappears at very forward rapidities. At midrapidity ($\eta = 0$), all three nPDFs yield a ratio that is essentially unity. The HKN07 nPDFs set manifests quantitatively a greater suppression at very backward rapidities, same as exhibited in d+Au collisions at RHIC.

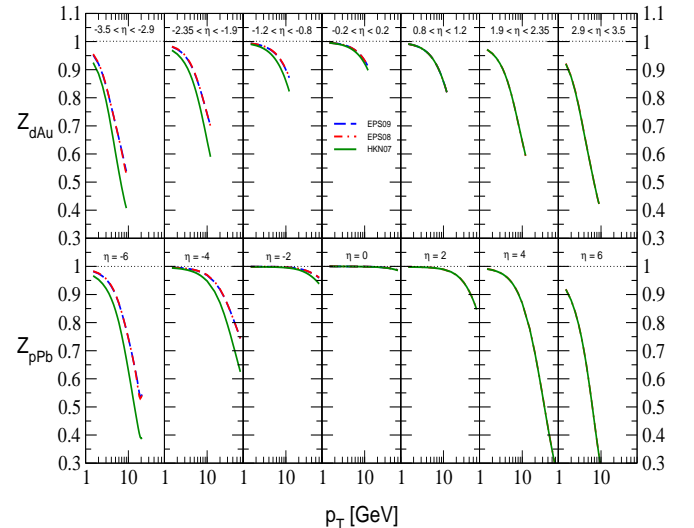


FIG. 5: (Color Online) Top panel: Charge ratio, Z_{dAu} , for charged hadron production in d+Au collisions at RHIC ($\sqrt{s_{NN}} = 200$ GeV) from backward ($\eta = -3.5$) to forward ($\eta = 3.5$) pseudorapidities. Bottom panel: Charge ratio, Z_{pPb} , for charged hadron production in p+Pb collisions at the LHC ($\sqrt{s_{NN}} = 8.8$ TeV) from backward ($\eta = -6$) to forward ($\eta = 6$) pseudorapidities. In general solid line represents the HKN07 nPDFs, dashed line the EPS09 nPDFs, while dot-dashed line represents the EPS08 nPDFs.

We now present the result for the pseudorapidity asymmetry of the charge ratio, Y_z^{AB} . As remarked above, this is just the ratio of the usual pseudorapidity asymmetry of negative hadrons relative to the positively charged hadrons. Since the charge ratio is close to unity around midrapidity, the focus of interest is the behavior at both very forward (small (large) x in target (projectile)) and backward (large (small) x in target (projectile)) rapidities. Thus the pseudorapidity asymmetry of the charge ratio helps to display the degree of asymmetry of the suppression relative to midrapidity.

In Figure 6 we display the asymmetry for d+Au collisions (top panel) and p+Pb collisions (bottom panel). For deuteron-gold collisions, the asymmetry is positive and increasing with increasing η for both EPS09 and EPS08. In the case of HKN07, the asymmetry is con-

sistent with unity for the first two η intervals, while it is slightly negative at large p_T for $2.9 < |\eta| < 3.5$. Let us

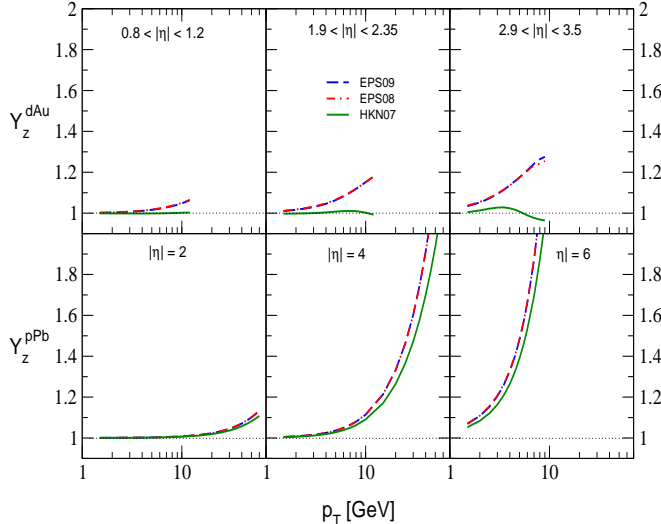


FIG. 6: (Color Online) Top panel: Pseudorapidity asymmetry of charge ratio, Y_z^{dAu} for charged hadrons at $0.8 < |\eta| < 1.2$, $1.9 < |\eta| < 2.35$, and $2.9 < |\eta| < 3.5$ from d+Au collisions at RHIC ($\sqrt{s_{NN}} = 200$ GeV). Bottom panel: Pseudorapidity asymmetry, Y_z^{pPb} for charged hadrons at $|\eta| = 2$, $|\eta| = 4$, and $|\eta| = 6$ from p+Pb collisions at the LHC ($\sqrt{s_{NN}} = 8.8$ TeV). In both cases the solid line represents the HKN07 nPDFs, the dashed line the EPS09 nPDFs, while the dot-dashed line represents the EPS08 nPDFs.

now consider p+Pb collisions at the LHC. Both EPS09 and EPS08 predict positive asymmetry for all rapidities considered, with the asymmetry increasing sharply with increasing η . This trend is replicated by the HKN07 set. The degree of asymmetry is consistent for all three sets at $|\eta| = 2$, with slight differences at high p_T for larger rapidities.

IV. CONCLUSION

In this study we have investigated the effects of different strengths of nuclear gluon modifications on charged

hadron production at both RHIC and the LHC, using three recent nuclear parton distributions. We considered asymmetric light-on-heavy systems where final-state effects (apart from fragmentations leading to final charged hadrons) are absent. The present treatment include observables like nuclear modification factor, pseudorapidity asymmetry, and charge ratio for both negative and positive pseudorapidity and up to relatively high transverse momenta, thereby ensuring adequate coverage of all relevant nuclear effects encoded in the nuclear parton distributions.

Each of the observables considered has its own strengths and weaknesses as a probe of nuclear effects in nuclear parton distributions. Nuclear modification factor probes directly nuclear effects for any p_T and at any pseudorapidity η . Its drawback is the dependence on knowledge of the requisite pp yield. The associated modification factor, central-to-peripheral ratio, while not dependent on the pp cross section, is geometry dependent. The pseudorapidity asymmetry, on the other hand, is independent of the pp cross section, but requires the cross section of p(d)A collisions at both forward and backward rapidities. It is thus somewhat less "clean" than the nuclear modification factor, but still has good potentials for constraining nPDFs. As shown above, the charge ratio is only sensitive in the backward region (large x in Au(Pb)); so it may offer some discriminating abilities for nuclear effects at large x .

While there are some clear differences between the predictions of the three nPDFs for the nuclear modification factor and pseudorapidity asymmetry at RHIC, the distinctions are significantly enhanced at the LHC, even up to relatively high transverse momenta. In particular, at very forward rapidities where nuclear shadowing is expected to dominate, the predictions of the nuclear modification factor for all three nPDFs are directly correlated with the strengths of their gluon modifications. This is also true for the predicted pseudorapidity asymmetries.

In conclusion, asymmetric p(d)A collisions, especially at the LHC, have great potential not only to shed light on the underlying dynamics of relativistic nuclear collisions, but also as a source of data to help better constrain nuclear gluon distributions.

V. ACKNOWLEDGMENTS

This work is supported in part by the NSF grant PHY0757839.

[1] K. J. Eskola, V. J. Kolhinen and C. A. Salgado, Eur. Phys. J. C **9**, 61 (1999).
[2] D. de Florian and R. Sassot, Phys. Rev. D **69**, 074028 (2004)
[3] M. Hirai, S. Kumano and T. H. Nagai, Phys. Rev. C **70**, 044905 (2004); Nucl. Phys. Proc. Suppl. **139**, 21 (2005).
[4] M. Hirai, S. Kumano and T. H. Nagai, Phys. Rev. C **76**, 065207 (2007)
[5] K. J. Eskola, H. Paukkunen and C. A. Salgado, JHEP **0807**, 102 (2008)

- [6] K. J. Eskola, H. Paukkunen and C. A. Salgado, JHEP **0904**, 065 (2009)
- [7] F. Gelis, E. Iancu, J. Jalilian-Marian and R. Venugopalan, arXiv:1002.0333 [hep-ph].
- [8] D. Kharzeev, E. Levin and M. Nardi, Nucl. Phys. A **730**, 448 (2004) [Erratum-ibid. A **743**, 329 (2004)].
- [9] M. Gyulassy, J. Phys. G **30**, S911 (2004).
- [10] T. K. Hemmick, J. Phys. G **30**, S659 (2004).
- [11] Cronin J W *et al* (CP Collaboration) 1975 *Phys. Rev. D* **11** 3105
- [12] Antreasyan D *et al* (CP Collaboration) 1979 *Phys. Rev. D* **19** 764
- [13] B. I. Abelev *et al.* [STAR Collaboration], Phys. Rev. C **76**, 054903 (2007); J. Adams *et al.* [STAR Collaboration], Phys. Rev. C **70**, 064907 (2004).
- [14] I. Arsene *et al.* [BRAHMS Collaboration], Phys. Rev. Lett. **93**, 242303 (2004).
- [15] P. Quiroga-Arias, J. G. Milhano and U. A. Wiedemann, arXiv:1002.2537 [hep-ph].
- [16] A. D. Martin, R. G. Roberts, W. J. Stirling and R. S. Thorne, Eur. Phys. J. C **4**, 463 (1998)
- [17] D. de Florian, R. Sassot and M. Stratmann, Phys. Rev. D **76**, 074033 (2007)
- [18] S. Albino, B. A. Kniehl and G. Kramer, Nucl. Phys. B **803**, 42 (2008)
- [19] N. Armesto, J. Phys. G **32**, R367 (2006)
- [20] D. Kharzeev, Y. V. Kovchegov and K. Tuchin, Phys. Lett. B **599**, 23 (2004)
- [21] V. Guzey, M. Strikman and W. Vogelsang, Phys. Lett. B **603**, 173 (2004)
- [22] R. C. Hwa, C. B. Yang and R. J. Fries, Phys. Rev. C **71**, 024902 (2005)
- [23] J. Nemchik, V. Petracek, I. K. Potashnikova and M. Sumbera, Phys. Rev. C **78**, 025213 (2008)
- [24] R. Vogt, Phys. Rev. C **70**, 064902 (2004).
- [25] P. Levai, G. G. Barnafoldi, G. Fai and G. Papp, Nucl. Phys. A **783**, 101 (2007).
- [26] A. Adeluyi and G. Fai, Phys. Rev. C **76**, 054904 (2007).
- [27] J. L. Albacete and C. Marquet, arXiv:1001.1378 [hep-ph].
- [28] A. Adeluyi, G. G. Barnafoldi, G. Fai and P. Levai, Phys. Rev. C **80**, 014903 (2009)
- [29] X. N. Wang, Phys. Lett. B **565**, 116 (2003).
- [30] G. G. Barnafoldi, P. Levai, G. Papp and G. Fai, Nucl. Phys. A **749**, 291 (2005).
- [31] G. G. Barnafoldi, A. Adeluyi, G. Fai, P. Levai and G. Papp, arXiv:0807.3384 [hep-ph].
- [32] I. Arsene *et al.* [BRAHMS Collaboration], Phys. Rev. Lett. **94**, 032301 (2005).
- [33] B. B. Back *et al.* [PHOBOS Collaboration], Phys. Rev. C **72**, 031901 (2005).